Environ Earth Sci (2017) 76:183
DOI 10.1007/s12665-017-6488-x

ORIGINAL ARTICLE

Seasonal disparity in the co-occurrence of arsenic and fluoride in the aquifers of the Brahmaputra flood plains, Northeast India

Nilotpal Das[1] · Kali P. Sarma[1] · Arbind K. Patel[1] · Jyoti P. Deka[1] · Aparna Das[1] · Abhay Kumar[2] · Patrick J. Shea[3] · Manish Kumar[1,4]

Received: 26 May 2016 / Accepted: 9 February 2017 / Published online: 22 February 2017

Abstract Arsenic (As) and fluoride (F^-) in groundwater are increasing global water quality and public health concerns. The present study provides a deeper understanding of the impact of seasonal change on the co-occurrence of As and F^-, as both contaminants vary with climatic patterns. Groundwater samples were collected in pre- and post-monsoon seasons ($n = 40$ in each season) from the Brahmaputra flood plains (BFP) in northeast India to study the effect of season on As and F^- levels. Weathering is a key hydrogeochemical process in the BFP and both silicate and carbonate weathering are enhanced in the post-monsoon season. The increase in carbonate weathering is linked to an elevation in pH during the post-monsoon season. A Piper diagram revealed that bicarbonate-type water, with Na^+, K^+, Ca^{2+}, and Mg^{2+} cations, is common in both seasons. Correlation between Cl^- and NO_3^- ($r = 0.74$, $p = 0.01$) in the post-monsoon indicates mobilization of anthropogenic deposits during the rainy season. As was within the 10 μg L^{-1} WHO limit for drinking water and F^- was under the 1.5 mg L^{-1} limit. A negative correlation between oxidation reduction potential and groundwater As in both seasons ($r = -0.26$ and -0.49, respectively, for pre-monsoon and post-monsoon, $p = 0.05$) indicates enhanced As levels due to prevailing reducing conditions. Reductive hydrolysis of Fe (hydr)oxides appears to be the predominant process of As release, consistent with a positive correlation between As and Fe in both seasons ($r = 0.75$ and 0.73 for pre- and post-monsoon seasons, respectively, at $p = 0.01$). Principal component analysis and hierarchical cluster analysis revealed grouping of Fe and As in both seasons. F^- and sulfate were also clustered during the pre-monsoon season, which could be due to their similar interactions with Fe (hydr)oxides. Higher As levels in the post-monsoon appears driven by the influx of water into the aquifer, which drives out oxygen and creates a more reducing condition suitable for reductive dissolution of Fe (hydr)oxides. An increase in pH promotes desorption of As oxyanions AsO_4^{3-} (arsenate) and AsO_3^{3-} (arsenite) from Fe (hydr)oxide surfaces. Fluoride appears mainly released from F^--bearing minerals, but Fe (hydr)oxides can be a secondary source of F^-, as suggested by the positive correlation between As and F^- in the pre-monsoon season.

Keywords Arsenic · Fluoride · Groundwater Quality · Hydrogeochemical process · Weathering · Brahmaputra River · India

Introduction

Arsenic in groundwater is a serious global concern. Most people worldwide depend on groundwater for drinking, irrigation and many other purposes. Inorganic As is toxic

Electronic supplementary material The online version of this article (doi:10.1007/s12665-017-6488-x) contains supplementary material, which is available to authorized users.

✉ Manish Kumar
manish.env@gmail.com

[1] Department of Environmental Science, Tezpur University, Napaam, Sonitpur, Tezpur, Assam 784-028, India

[2] Central Institute of Educational Technology (CIET), National Council of Educational Research and Training (NCERT), New Delhi 110016, India

[3] School of Natural Resources, University of Nebraska-Lincoln, 102 Kiesselbach, PO Box 830817, Lincoln, NE 68583-0817, USA

[4] Present Address: Department of Civil Engineering, University of Nebraska-Lincoln, N125 Scott Engineering Center Link, Lincoln, NE 68588-6105, USA

and consuming high doses can be fatal. Long-term chronic exposure may lead to cancer or degenerative effects on the circulatory and nervous systems (Liao et al. 2008; Halim et al. 2010). In Bangladesh and West Bengal, India, a switch from surface to groundwater since the second half of the last century has contributed significantly to As-related health hazards (Harvey et al. 2005). The eastern Indian subcontinent, including Bangladesh and Indian parts of the Indo-Gangetic Plains, and especially West Bengal, are reported major hotspots of As contamination. Other countries affected by groundwater As contamination include Vietnam, Cambodia, China, Nepal, Argentina, Chile, Mexico, and the USA (Bhattacharya et al. 2002, 2003; Smedley and Kinniburgh 2002; Smedley et al. 2002, 2003; Bundschuh et al. 2004; Ahmed et al. 2004; Kumar et al. 2010a, b).

High As has been reported in groundwater of northeast India, including Assam (Ghosh and Singh 2009). High As and Fe were reported in the Tamarhat and Paglahat in the Dhubri district and As levels in the Charkhola area of Bongaigaon have exceeded the WHO (WHO 2008) permissible limit of 10 μgL^{-1} (Reddy 2012). The North East Regional Institute of Water and Land Management (NERIWALM), Tezpur, Assam, India, reported As as high as 117 $\mu g\ L^{-1}$ in groundwater of the State of Tripura in northeast India (Singh 2004). Reports from other parts of Assam indicate similar findings (Singh 2004; Mukherjee et al. 2006; Bhuyan and Bhuyan 2011). However, these studies did not explore the hydrogeochemistry associated with the As contamination and mobilization.

High concentrations of F^- (>1.5 mg L^{-1}) is another serious groundwater concern (WHO 2008; Brindha et al. 2011). Globally, as many as 25 million people suffer health disorders due to consumption of F^--contaminated groundwater (Brindha et al. 2011). Fluorosis has been reported around the world and North and South America, Africa, Middle Eastern countries, India, and China are some of the most affected regions (Brunt et al. 2004). In India, high groundwater F^- has been reported in southern and western states (Andhra Pradesh, Bihar, Gujarat, Madhya Pradesh, Punjab, Rajasthan, Tamil Nadu, and Uttar Pradesh) (Pillai and Stanley 2002; Brindha et al. 2011). Adverse health effects related to consuming groundwater high in F^-, such as dental and skeletal fluorosis, are prevalent in these regions, and more than 62 million people in India are reportedly at risk (Brindha et al. 2011).

High levels of F^- were discovered in the groundwater of the northeast Indian state of Assam in the 1990s (Singh 2004). In Assam, very high groundwater F^- (up to 20.6 mg L^{-1}) has been reported in the districts of Karbi Anglong and Nagaon (Chakraborti et al. 2000; Susheela 2001). The situation in Karbi Anglong has been reported as critical; in 2000 more than 640 people were identified with dental fluorosis and 36 with skeletal fluorosis (Chakraborti et al. 2000). The number of people affected is expected to increase with time. High F^- groundwater has been found in urban areas such as Guwahati, the capital and economic hub of the Assam region (Das et al. 2003). However, research pertaining to F^- in northeast India is limited.

High fluoride concentrations typically occur in aquifers where groundwater has a long residence time, as mineral dissolution has been reported to be the primary mode of F^- mobilization (Saxena and Ahmed 2001, 2003; Brunt et al. 2004). Therefore, elevated levels of F^- have been found mainly in arid to semiarid areas where groundwater recharge is very slow (Brunt et al. 2004; Arveti et al. 2011; Brindha et al. 2011). This is true in India, as high groundwater F^- is found in many arid to semiarid regions of the country. However, the average annual rainfall in northeast India is very high and most of northern Assam is dominated by a fluvial environment due to the presence of the Brahmaputra flood plains (BFP). Because the climatic and the environmental conditions of Assam and the rest of northeast India appear unsuitable for F^- in groundwater, localized F^- in groundwater of Assam is likely due to other factors, which are examined here.

The BFP is a vast region with a very high population density. There is much variability in the distribution of As and F^- in the groundwater of this region and the associated hydrogeochemistry is not well understood. The present study provides a deeper understanding of the impact of seasonal change on the co-occurrence of As and F^- and their hydrogeochemical mobilization in aquifers of the BFP.

The Brahmaputra flood plains (BFP) study area

The BFP is said to be of tectonic origin; the valley portion was formed by compression between the European and the Indian plate, which also led to formation of the Himalayan Mountains (Mithal and Srivastava 1959; Evans 1964; Tapponier and Molnar 1977; Mahanta 1995). The main type of sediment in the BFP is undifferentiated alluvium deposited over successive periods of sedimentation (Fig. 1). Sediment characteristics vary based on the origins and features of the northern and southern tributaries (Mahanta 1995). The larger northern tributaries, of Himalayan origin, have greater sediment discharge, consisting mainly of silt fractions (Mahanta 1995). The beds and the banks of the southern tributaries were formed by non-alluvial sediments (Mahanta 1995).

Soils of the BFP are classified based on mode of formation as residual or transported (Mahanta 1995). Residual soils formed in situ from the parent rocks of the Archaean age, consisting mainly of gneisses, schists, and granites (Mahanta 1995), while transported soils formed through weathering of rocks of the Himalayas and the Assam plateau (Mahanta 1995). The spatial distribution of soil types shows

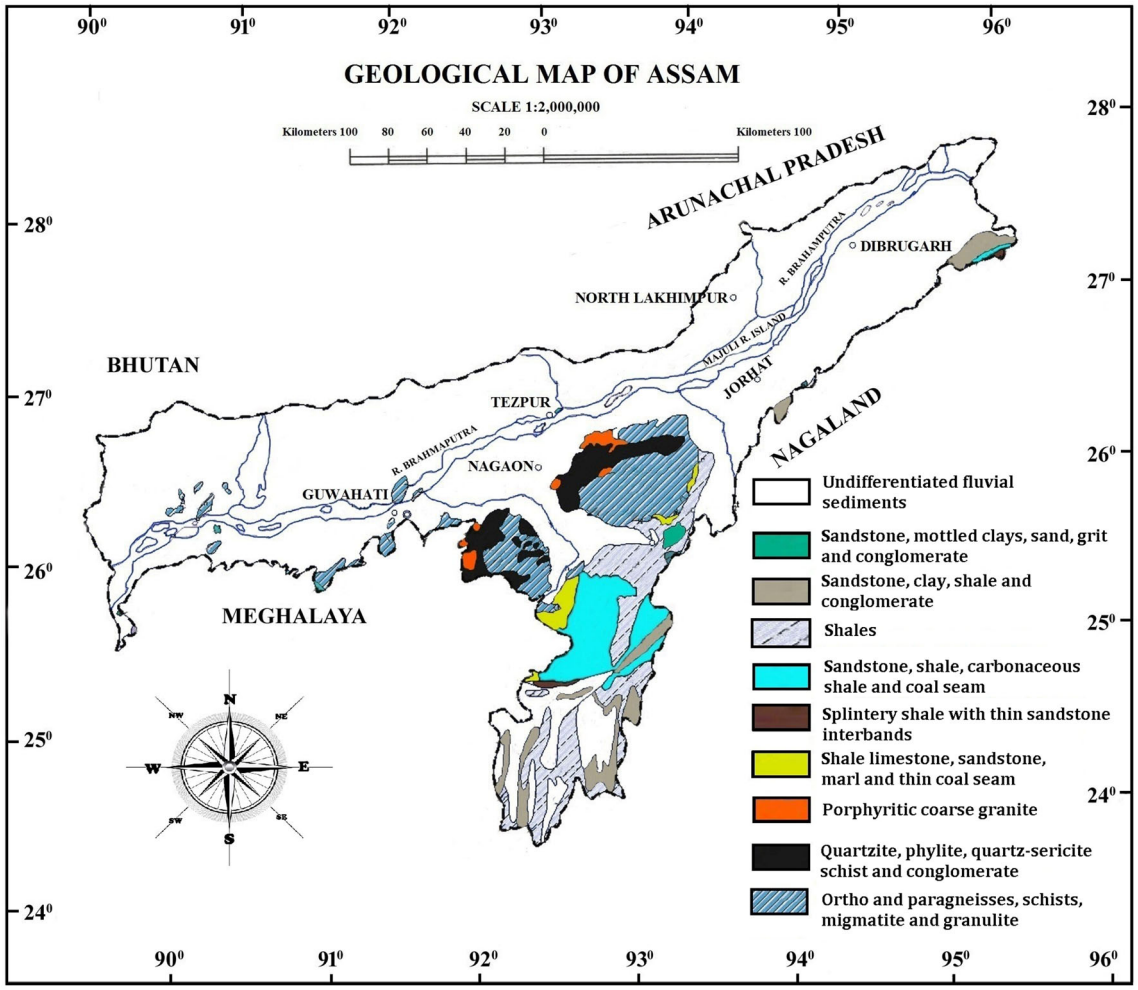

Fig. 1 Geological base map of Assam modified from Geological Survey of India showing the different geological formations

that alluvium formed along recent river deposits and occurs in the valley region. Older alluvium occurs in the piedmont or uplands regions (Mahanta 1995). Repeated sequencing of clay, fine sand, coarse sand with cobbles, pebbles, and boulders has been found in borings up to 100 m below ground level (Balasundaram 1977; Mahanta 1995).

The river Brahmaputra and its Himalayan tributaries have been flowing through and weathering a number of different rock types, including "Precambrian metamorphics (high-grade schists, gneisses, quartzites, metamorphosed limestones), felsic intrusive, and Paleozoic–Mesozoic sandstones, shales and limestones" (Huizing 1971; Heroy et al. 2003). The BFP is divided into two distinct hydrogeological regions: the dissected alluvial plains and the inselberg zone (Jain et al. 2007). The dissected alluvial region extends from the south of the lower Himalayan piedmont fan zones to the "main rock promontory" of the Garo hills and Shillong plateau in the south (Mahanta 1995). Groundwater occurrence is controlled by deformities such as "foliations, fractures/joints and weathered zones" in the "hard rock inselberg region." The groundwater has a southerly slope, corresponding to surface topography.

Materials and methods

Sampling and analysis

Forty groundwater samples were collected from the BFP study area in the pre-monsoon (February) and post-monsoon (September) seasons of 2011 (Fig. 2). Sampling site coordinates were noted using a handheld GPS set (Garmin GPS map 76CSX). Groundwater was sampled following the method of Critto et al. (2003). All samples were collected from tube wells. Purging was performed for about 5 min to remove stagnant or residual water from the tube, manually pumping until specific conductance, temperature and the pH stabilized. Samples were stored in polyethylene bottles after rinsing them 2–3 times with the water to be

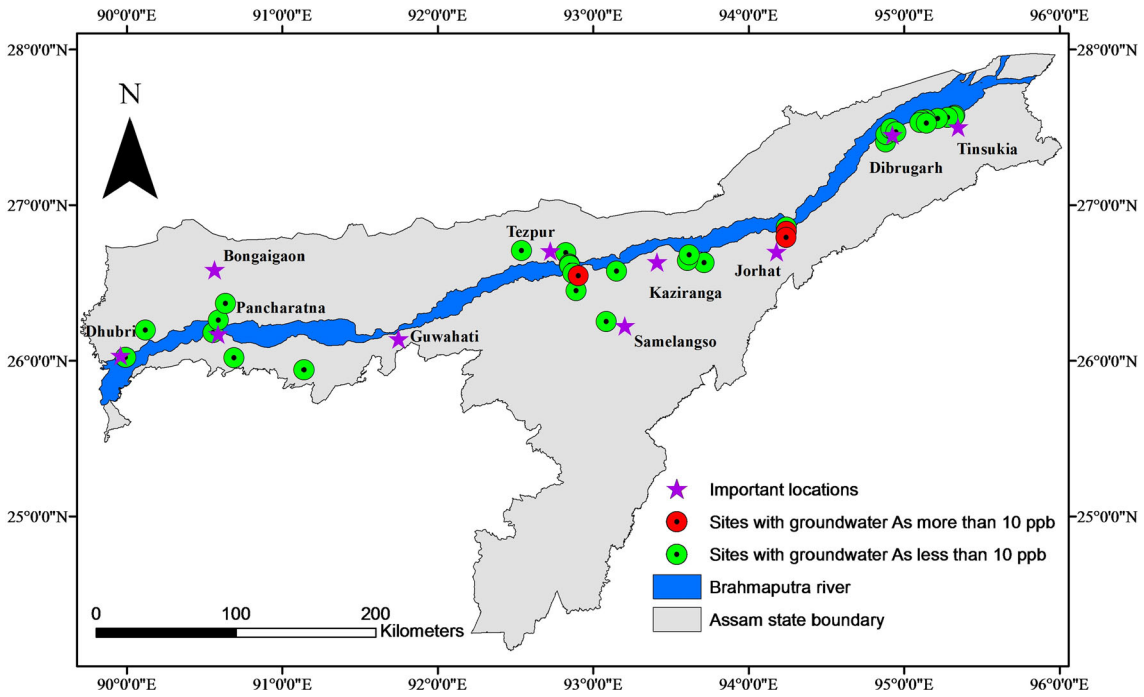

Fig. 2 Map of the study area (BFP) showing places of importance along with sediment and groundwater sampling locations

sampled. For cations, Fe and As analyses, the groundwater was filtered through Millipore (0.45-μm) filters and acidified with 16 N HNO_3 to reduce the pH to ≤ 2. For anion analysis, raw unfiltered samples were collected; precautions were taken to avoid headspace in the bottles. The collected samples were stored at 4 °C until analysis.

Electrical conductivity (EC), pH, dissolved oxygen (DO), oxidation reduction potential (ORP), and total dissolved solids (TDS) were measured onsite using a multiparameter probe (HANNA HI9828). Na^+, K^+, and Ca^{2+} were determined by flame photometry (Systronics Flamephotometer 128); and Mg^{2+} and Fe by inductively coupled plasma optical emission spectroscopy (ICP-OES, PerkinElmer Optima DV2100). Arsenic was determined using atomic absorption spectroscopy (AAS, Thermo Scientific ICE 3000). SO_4^{2-}, PO_4^{3-} and H_4SiO_4 were measured by UV spectrophotometry (Shimadzu, UV-1700), following American Public Health Association methodology (APHA 2005). HCO_3^- was determined by potentiometric titration and Cl^- by the argentometric method (APHA 2005). Accuracy of the analytical methods was checked by calculating inorganic charge balance:

$$\text{Inorganic charge balance} = \frac{Tz^+ - Tz^-}{Tz^+ + Tz^-}$$

where Tz^+ and Tz^- are total cations and total anions, respectively (Chen et al. 2007). The charge balance of the data was within 5% variance. Statistical analysis was performed using SPSS 20 and included correlation, hierarchical cluster (HCA) and principal component (PCA) analyses. Speciation modeling was conducted using MINTEQA2 v 3.1.

Results and discussion

Hydrogeochemistry

The hydrogeochemical characteristics of the BFP study are summarized in Table 1. Piper diagrams (Piper 1953) were prepared to observe seasonal variations in hydrological facies. Bicarbonate (HCO_3^-) type water, with mixed contributions from the cations Na^+, K^+, Ca^{2+}, and Mg^{2+}, appears common in both pre- and post-monsoon seasons (Fig. 3a, b). However, closer observation reveals that HCO_3^- type water is more common in the post-monsoon. High As was associated with HCO_3^--type water in both pre- and post-monsoon seasons, indicating the influence of an alkaline environment in enhancing groundwater As levels.

A preliminary investigation of hydrogeochemical processes in the aquifers of the study area was conducted by constructing Gibbs plots (Fig. 4) (Fisher and Mullican 1997) which suggest that weathering and dissolution processes are the dominant groundwater processes in the area. The influences of rock dominance, evaporation, and precipitation can be identified from the Fig. 4a and b based on total dissolved solids (TDS) versus $(Na^+ + K^+)$/

Table 1 Descriptive statistics of the hydrochemical parameters spatially and seasonally

Parameter	Unit	Pre-monsoon			Post-monsoon		
		Range	Mean	SD	Range	Mean	SD
TDS	mgL^{-1}	21.5–375	137	81.8	29.9–783	172	133
pH		5.04–7.24	6.29	0.54	6.18–10.2	7.53	0.71
ORP	mV	−136–(−185)	5.8	60.1	−115–(−126)	−13.3	44.8
EC	µS/cm	43.4–400	206	90.1	61.3–1586	299	246
Na^+	mgL^{-1}	3.4–38	12.3	7.93	0.96–41.5	16.6	11.07
K^+	mgL^{-1}	0.3–14	2.37	2.62	0.11–13.9	3.02	2.75
Ca^{2+}	mgL^{-1}	5.6–119	26.1	21.1	3.12–85	21.9	17.6
Mg^{2+}	mgL^{-1}	2.38–27.5	8.98	6.69	2.53–35.5	8.66	7.05
Cl−	mgL^{-1}	5.68–88	25.8	17.7	5.68–332	37.5	50.8
SO_4^{2}−	mgL^{-1}	6.1–103	13.4	16.7	0.03–142	14.6	24.7
PO_4^{3}−	mgL^{-1}	0.16–1.83	0.52	0.4	0.16–2.56	0.39	0.42
NO_3−	mgL^{-1}	ND–2.01	0.44	0.53	ND–1.96	0.33	0.36
HCO_3−	mgL^{-1}	55–400	167	91.2	5–400	188	87.6
F−	mgL^{-1}	ND–14.4	0.50	2.35	ND–0.45	0.085	0.14
As	μgL^{-1}	0.18–22.1	2.6	3.85	0.78–17.3	4.13	3.59
Fe	mgL^{-1}	0.01–2.89	0.44	0.7	0.02–8.08	1.75	1.47

ND not detectible

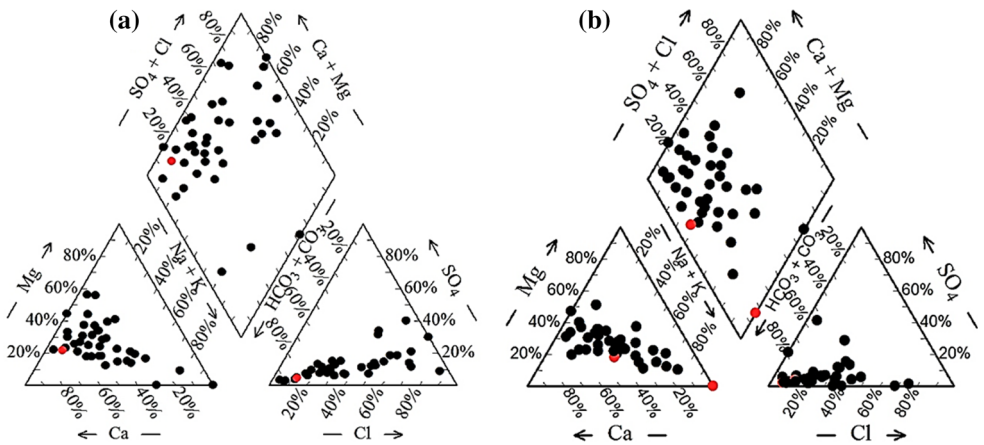

Fig. 3 Piper diagram showing the different groundwater types in the **a** pre-monsoon and **b** post-monsoon seasons. *Note*: The *red solid circles* indicate groundwater samples with As level >10 μgL^{-}

$(Na^+ + K^+ + Ca^{2+})$ and TDS versus $Cl^-/(Cl^+ + HCO_3^-)$ (Gibbs 1970).

In the pre-monsoon season, both evaporation and salt dissolution play an important role in controlling the hydrochemistry of the region; this is evident from the positive relationship between TDS and Cl^- ($r = 0.74$, $p = 0.01$) (Table 2). TDS also showed moderate relationships with EC, K^+ and SO_4^{2-} ($r = 0.57$, 0.74 and 0.54 respectively at $p = 0.05$). In an aquatic system, pH and HCO_3^- are interdependent and the two parameters were positively ($r = 0.52$, $p = 0.05$) associated in the pre-monsoon season. The pH and ORP were negatively correlated ($r = 0.78$, $p = 0.01$) in the pre-monsoon season. Fe and ORP were weakly correlated ($r = -0.43$, $p = 0.05$), which could be due to the prevalence of reductive hydrolytic processes in the pre-monsoon. Silicate weathering could account for the moderate positive correlation between EC and K^+ ($r = 0.52$, $p = 0.05$) in the pre-monsoon. Pre-monsoon weathering of dolomite can explain the positive relation between Ca^{2+} and Mg^{2+} ($r = 0.66$, $p = 0.05$). Both SO_4^{2-} and Cl^- anions are likely responsible for permanent hardness in the groundwater and anthropogenic factors could account for their moderate positive association ($r = 0.54$, $p = 0.05$).

Higher TDS in the post-monsoon season suggests more weathering and dissolution than in pre-monsoon. The pH is higher in post-monsoon than in the pre-monsoon season, likely due to more carbonate dissolution leading to an increase in HCO_3^-. The prevalence of reducing and oxidizing conditions in both seasons indicates the presence of

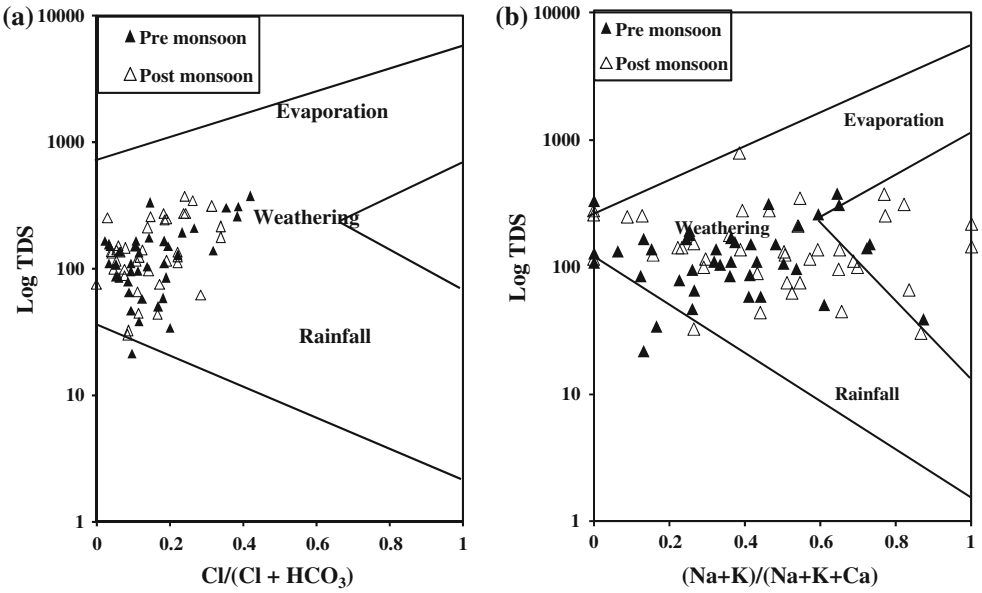

Fig. 4 Gibbs plots showing that rock–water interaction controls the groundwater chemistry **a** and **b** seasonally

Table 2 Correlation matrix for pre-monsoon season

	TDS	pH	ORP	EC	Na^+	K^+	Ca^{2+}	Mg^{2+}	Cl^-	SO_4^{2-}	PO_4^{3-}	NO_3^-	HCO_3^-	F^-	As
pH	0.17														
ORP	−0.11	**−0.78**													
EC	**0.57**	0.39	−0.27												
Na^+	0.38	0.05	0.05	−0.03											
K^+	**0.64**	−0.06	−0.02	**0.52**	0.29										
Ca^{2+}	0.02	0.14	−0.09	0.06	−0.31	0.02									
Mg^{2+}	0.00	0.34	−0.28	0.26	−0.41	−0.10	**0.66**								
Cl^-	**0.74**	−0.06	0.10	0.25	0.37	0.41	−0.03	−0.16							
SO_4^{2-}	**0.54**	0.18	−0.08	0.14	0.34	0.23	−0.08	−0.09	**0.54**						
PO_4^{3-}	0.09	0.30	−0.29	0.25	−0.07	0.10	0.18	0.39	−0.20	0.04					
NO_3^-	0.42	−0.08	0.13	0.14	0.20	0.06	−0.07	−0.04	**0.59**	0.12	−0.27				
HCO_3^-	0.12	**0.52**	−0.39	0.36	0.04	−0.15	0.19	0.21	−0.08	0.20	0.05	0.02			
F^-	0.44	0.23	−0.20	0.11	0.09	0.14	−0.11	0.17	0.26	**0.86**	0.00	−0.05	0.29		
As	0.14	0.25	−0.26	0.28	−0.17	0.10	0.01	−0.03	−0.05	0.04	−0.06	−0.03	0.39	0.13	
Fe	0.12	0.42	−0.43	0.35	0.06	0.05	0.04	0.29	−0.13	−0.05	0.08	0.11	0.45	0.50	**0.75**

Bold indicates significant loading

a mixed aquifer system. However, reducing conditions were more common than oxidizing conditions (Supplemental Fig. 1). TDS and Cl^- are more strongly correlated ($r = 0.86$, $p = 0.01$) in the post-monsoon season (Table 3), due to greater salt weathering and dissolution than in the pre-monsoon. TDS was also correlated with EC ($r = 0.93$, $p = 0.01$) in the post-monsoon. Positive correlations between TDS and NO_3^- ($r = 0.74$, $p = 0.01$), and EC and NO_3^-($r = 0.71$, $p = 0.01$), can be attributed to greater anthropogenic inputs from non-point sources in the post-monsoon. The correlation between Cl^- and NO_3^-($r = 0.74$, $p = 0.01$) confirms more anthropogenic input in the post-monsoon season and residual pollutants may also be mobilized. The correlation between Ca^{2+} and Mg^{2+} ($r = 0.86$, $p = 0.01$) is stronger in the post-monsoon than in the pre-monsoon season when more weathering of dolomite occurs. The negative correlation between Fe and ORP ($r = -0.12$) in the post-monsoon season, reflected the predominantly reducing environment of the BFP.

Weathering and dissolution are important hydrogeochemical processes during both pre- and post-monsoon seasons. The contribution to silicate and carbonate weathering can be evaluated by plotting total cations (Tz^+) versus (Na^++K^+) and (Ca^{2+}+Mg^{2+}) (Fig. 5a, b).

Table 3 Correlation matrix for post-monsoon season

	TDS	pH	ORP	EC	Na^+	K^+	Ca^{2+}	Mg^{2+}	Cl^-	SO_4^{2-}	PO_4^{3-}	NO_3^-	HCO_3^-	F^-	As
pH	0.18														
ORP	−0.06	−0.12													
EC	**0.93**	0.10	−0.09												
Na^+	−0.07	0.06	0.02	−0.13											
K^+	0.14	0.15	0.17	0.11	0.39										
Ca^{2+}	0.08	−0.04	−0.12	0.13	−0.24	−0.15									
Mg^{2+}	0.07	0.05	−0.06	0.12	−0.13	0.00	**0.86**								
Cl^-	**0.86**	0.05	0.00	**0.89**	−0.03	0.09	−0.08	−0.06							
SO_4^{2-}	0.09	−0.00	−0.02	0.05	−0.02	−0.03	−0.07	−0.12	−0.01						
PO_4^{3-}	−0.14	−0.07	0.23	−0.10	0.01	0.08	−0.07	−0.07	−0.13	−0.08					
NO_3^-	**0.74**	0.01	0.13	**0.71**	0.01	0.10	−0.03	0.04	**0.74**	−0.02	−0.05				
HCO_3^-	0.05	0.44	−0.13	0.03	0.12	0.04	0.09	0.09	−0.02	0.18	0.26	0.01			
F^-	0.15	−0.12	0.08	0.13	0.02	0.04	−0.27	−0.26	0.30	−0.13	0.03	0.26	−0.12		
As	−0.06	0.11	−0.49	0.02	0.08	−0.14	0.08	−0.07	−0.14	−0.03	0.06	−0.05	0.22	−0.13	
Fe	0.16	−0.00	−0.12	0.31	0.08	−0.12	0.02	−0.06	0.23	0.00	0.03	0.27	0.15	0.31	**0.73**

Bold indicates significant loading

Carbonate weathering appeared dominant, as $Ca^{2+}+Mg^{2+}$ loadings were closer to the 1:1 line than were Na^++K^+ loadings (Kumar et al. 2008). The Na^+/Cl^- ratio is an important indicator of hydrochemical processes. A ratio close to 1 indicates halite dissolution; ratios <1 (higher Cl^-) indicate evapotranspiration, coupled with reverse ion exchange of Na^+ with Ca^{2+}, and ratios >1 (higher Na^+) indicate silica weathering (Kumar et al. 2006, 2008). Pre- and post-monsoon trends were similar (Fig. 5c), as both evapotranspiration and halite dissolution were important processes in both seasons. Na^+/Cl^- ratios show wide variation with increasing EC (Fig. 5c), which indicates high ionic activities like ion exchange and weathering and dissolution (Kumar et al. 2006, 2008). The next diagram (Fig. 5d), however, shows more samples with ratios above the 1:1 line in the post-monsoon season, implying greater silicate weathering due to precipitation (Rajmohan and Elango 2004; Kumar et al. 2008). Probable silicate minerals involved in Na^+ and K^+ release into groundwater include albite (soda feldspar) and, orthoclase and microline (potash feldspar). Feldspar is suggested rather than quartz because quartz is more resistant to weathering and changes in silicate rocks (Kumar et al. 2008).

Sources of NO_3^- and K^+ appear different, as K^+ is much greater than NO_3^- and no relation was observed between the two (Fig. 5e). This indicates that silicate weathering is the likely source of K^+, while NO_3^- is primarily due to anthropogenic inputs (Kumar et al. 2006). NO_3^- was very low in BFP groundwater. NO_3^- can be an oxygen donor for bacterial degradation of organic matter, leading to reducing conditions in the aquifers. Although the negative ORPs of most of the groundwater samples indicate reducing conditions, it is unlikely that NO_3^- is driving As release as NO_3^- was quite low in both pre- and post-monsoon seasons (Table 1). The same observation was made for NO_3^- in both seasons. A plot of NO_3^- versus Cl^- (Fig. 5f) shows a positive relationship between Cl^- and NO_3^-, which could be due to their similar origins, i.e., anthropogenic wastes. The association is stronger during the post-monsoon season (Fig. 5f), which could be due to mobilization of the anthropogenic deposits of the previous season.

The Ca^{2+}/Mg^{2+} ratio is an indicator of calcite and dolomite dissolution (Kumar et al. 2006). Calcite weathering is predominant in the post-monsoon season (Fig. 6a). This could be due to increased weathering and dissolution brought about by precipitation. A plot of $Ca^{2+}+Mg^{2+}$ versus $SO_4^{2-}+HCO_3^-$ (Fig. 6b) further supports enhanced carbonate weathering in the post-monsoon season, as more sample ratios lie below the 1:1 line (Kumar et al. 2006, 2008). Reverse ion exchange was slightly more common in the pre-monsoon (Fig. 6b), likely because in the post-monsoon it is diminished further by precipitation-induced carbonate weathering. Plots of $Ca^{2+}+Mg^{2+}$ versus Cl^- (Fig. 6c) do not show significant trends in either season, which indicates sources of $Ca^{2+}+Mg^{2+}$ and Cl^- are different. Much of the Cl^- may be from anthropogenic sources.

The source of Ca^{2+} in the groundwater was studied further using plots of Ca^{2+} versus HCO_3^-. Most of the samples fall above the 1:1 line near the region where the Ca^{2+}:-HCO_3^- ratio approaches 1:2 (Fig. 6d) (Kumar et al. 2008), indicating the dominance of carbonate weathering. This is confirmed by a plot of Ca^{2+} versus SO_4^{2-} (Fig. 6e) in which most of the samples from both seasons are below the 1:2 line. Thus Ca^{2+} increases without an increase in SO_4^{2-},

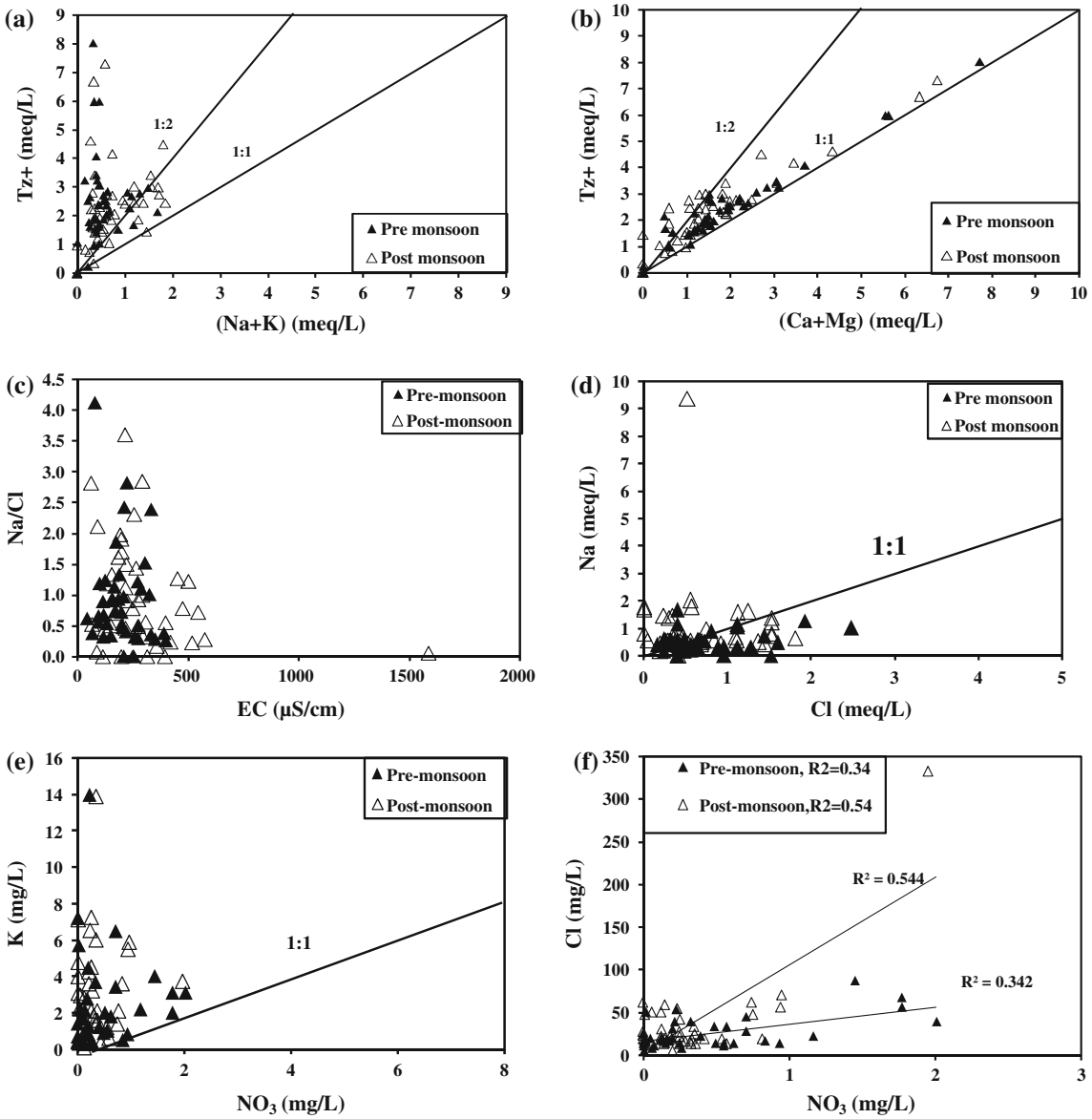

Fig. 5 Scatter plots for investigating the hydrochemistry of the pre- and post-monsoon. **a** Tz^+ versus (Na^++K^-), **b** Tz^+ versus (Ca^{2+}+Mg^{2+}), **c** (Na+/Cl−) molar ratio versus EC, **d** Na^+ versus Cl^-, **e** K^+ versus NO_3^- and **f** Cl^- versus NO_3^-

indicating calcite weathering as the probable source of Ca^{2+} rather than gypsum (Das and Kaur 2001; Kumar et al. 2008).

A plot of (Ca^{2+}+Mg^{2+})/HCO_3^- versus Cl^- shows that (Ca^{2+}+Mg^{2+})/HCO_3^- ratio does not increase with increasing salinity (Reddy et al. 2010). Thus Ca^{2+} and $Mg^{2+}$are added at a much slower rate than HCO_3^- throughout the year (Fig. 6f). Calcite weathering is the source of Ca^{2+} in our study area. If the opposite had been observed, silicate weathering would predominate.

Arsenic and fluoride

Most of the groundwater samples in this study had As values within the 10 µg L^{-1} WHO limit for drinking water (WHO 2008). The highest groundwater As level (22.1 µg L^{-1}) was found during the pre-monsoon season in a 13.7-m-deep tube well in the Naltali area of the Nagaon district, south of Tezpur. In the post-monsoon, two groundwater samples in the Jorhat District, each at approximately 30 m depth, contained 17.3 and 16.74 µg As L^{-1}. No clear trend between As and sampling depth was observed in the BFP study area. For samples with As levels within the permissible limit, the As level decreased with depth in the post-monsoon season, but there was no relationship in the pre-monsoon (Fig. 7a). The reducing condition prevalent in the BFP is evident from the largely negative ORPs of the region (Table 1). ORP and groundwater As levels were negatively correlated in both pre- and post-monsoon

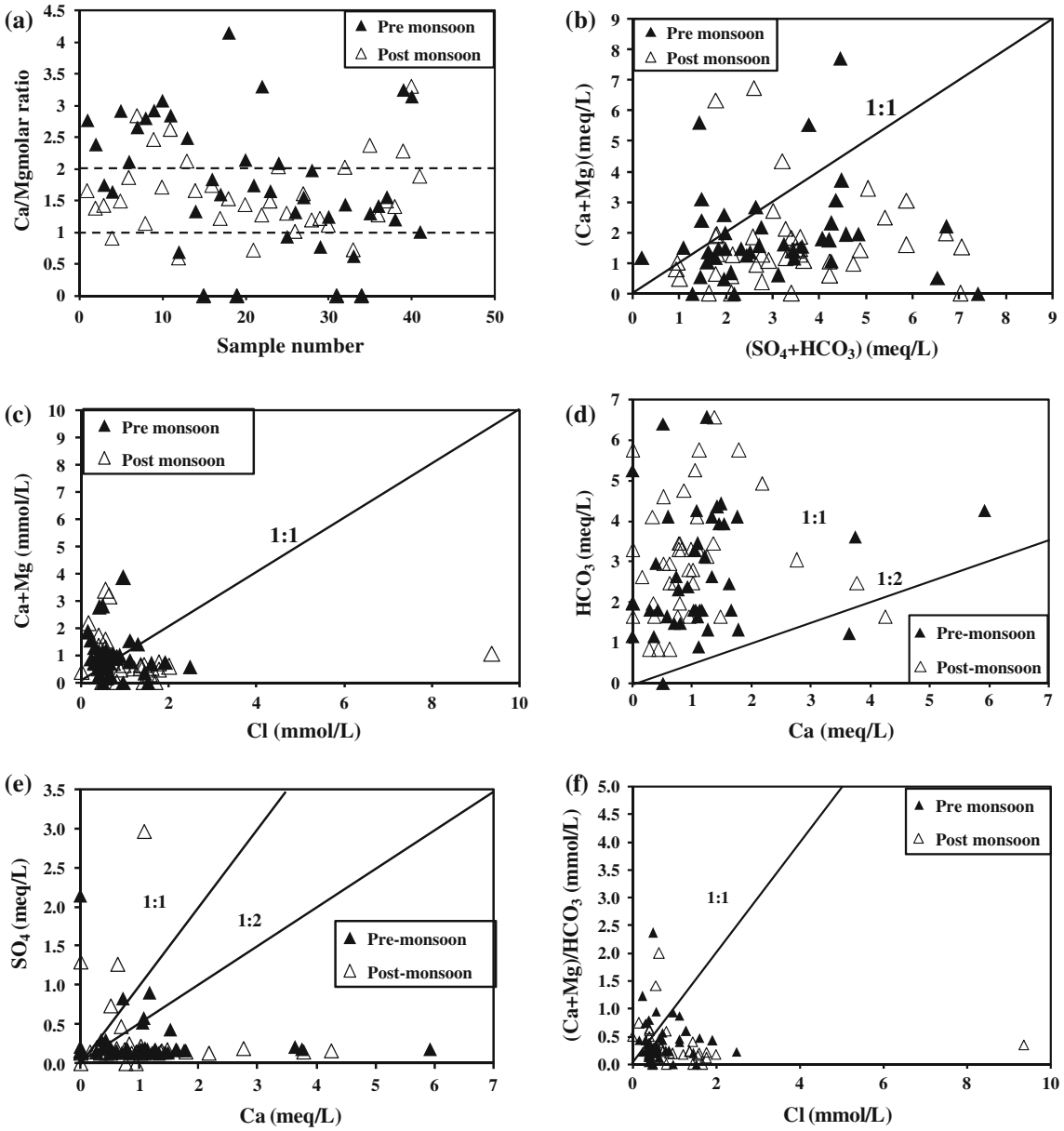

Fig. 6 Scatter plots for investigating the seasonal trends of carbonate weathering in the BFP **a** (Ca^{2+}/Mg^{2+}) versus Sample No. **b** (Ca^{2+}/Mg^{2+}) versus (SO_4^{2-}/HCO_3^-) **c** (Ca^{2+}/Mg^{2+}) versus Cl^- **d** HCO_3^- versus Ca^{2+} **e** SO_4^{2-} versus Ca^{2+} **f** (Ca^{2+}/Mg^{2+})/HCO_3^- versus Cl^-

seasons (Fig. 7b). This indicates groundwater As enhancement due to the prevailing reducing conditions. While both pH and ORP can influence As release in groundwater (Smedley and Kinniburgh 2002; Kim et al. 2012), neither were correlated with As levels in the pre-monsoon. The relationship between As and Fe ($r = 0.73$, $p = 0.01$) suggests an association of As levels with reductive hydrolysis of Fe (hydr)oxides (Fig. 7c). Correlation analysis also showed good correlation of As with Fe during both pre- and post-monsoon seasons (Tables 2, 3). This supports reductive hydrolysis of Fe (hydr)oxides as the principal mode of As mobilization in the BFP throughout the year. While a strong association was not observed between As and pH, it appears that As mobilization increases with pH (Fig. 7d). An increase in pH has been linked to desorption of As oxyanions from surfaces with a pH-dependent charge, such as Fe (hydr)oxides (Kim et al. 2012). Maximum desorption occurs at pH levels above the point of zero charge (Smedley and Kinniburgh 2002; Kim et al. 2012).

In contrast to As, seasonal variations did not greatly affect F^- mobilization in the BFP. Due to the low levels of F^-, scatter plots (Fig. 8a) yielded inconclusive results. There was no variation with depth. Fluoride appears prevalent under both reducing and oxidizing conditions and a slight negative correlation was observed between

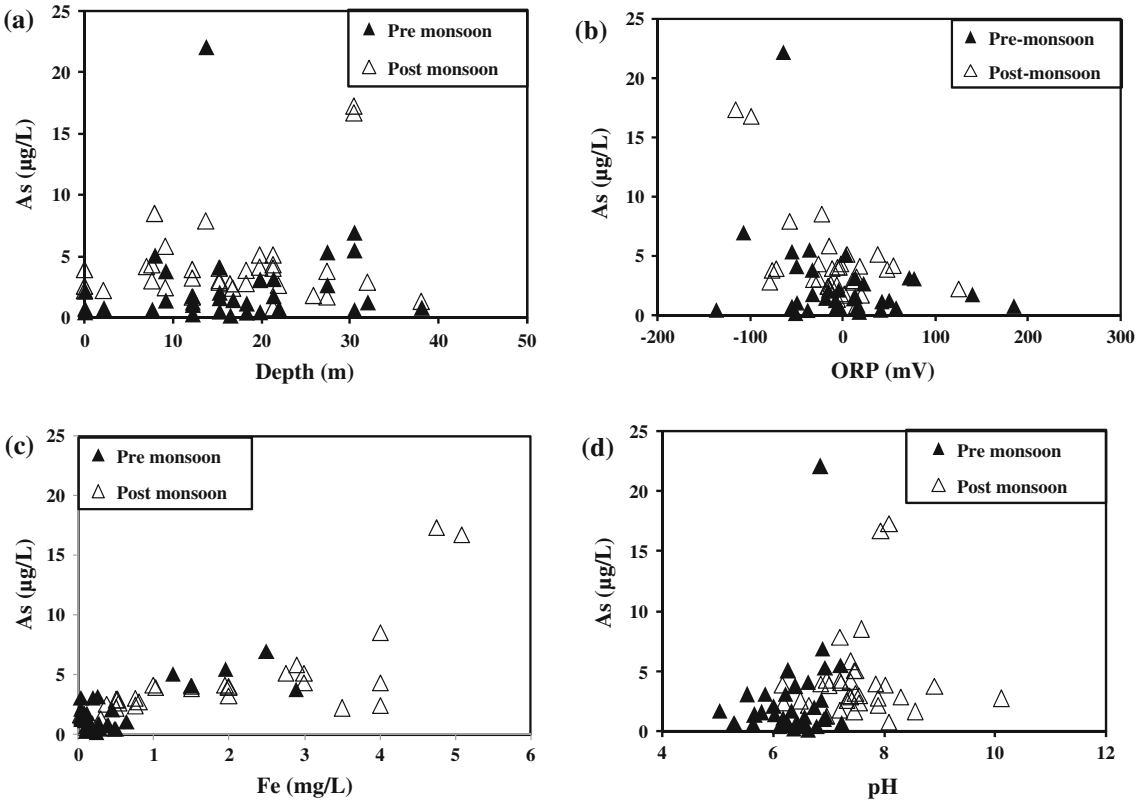

Fig. 7 Comparison of As behavior with other parameters spatially and seasonally. **a** As versus depth, **b** As versus ORP, **c** As versus Fe, **d** As versus pH

groundwater F^- and ORP (Fig. 8b). However, unlike As, F^- levels were not associated with Fe in groundwater (Fig. 8c). While F^- levels have been reported to increase with pH and an alkaline condition (Saxena and Ahmed 2001, 2003), no clear association was observed in our study (Fig. 8d. In the pre-monsoon season SO_4^{2-} and F^- exhibit a very strong correlation ($r = 0.86$, $p = 0.01$) (Table 2) which could be due to their common origin and release during hydrolysis of the Fe (hydr)oxides holding them. This relationship was explored further using multivariate analyses.

Principal component analysis

PCA identified three components explaining 80.8 and 74.5% of the overall variance for all measured parameters in the pre- and post-monsoon seasons, respectively (Table 4). In the pre-monsoon season, the first PC accounted for 40.9% of the variance and includes positive loadings by TDS, pH, EC, K^+, Cl^-, HCO_3^-, As and Fe, and negative loading by ORP. This PC appears controlled by weathering/dissolution and reductive hydrolytic processes, based on high loadings of As and Fe. High loading of pH and HCO_3^- reflects an alkaline environment which promotes As desorption from the Fe (hydr)oxides (Smedley and Kinniburgh 2002; Kim et al. 2012; Kumar et al. 2010b). TDS and EC loaded highly and are strongly influenced by evaporative processes. The second PC in the pre-monsoon accounts for 22.5% of the overall variance, with high loading by Ca^{2+}, Mg^{2+}, SO_4^{2-} and F^-. The process of silicate and carbonate weathering could be a major influence on this PC, resulting in release of Ca^{2+} and Mg^{2+}. Although SO_4^{2-} has a high loading on this component, it is unlikely to represent gypsum dissolution, as graphical inference (Fig. 6e) indicates carbonate rather than gypsum weathering. The high loading of SO_4^{2-} and F^- could represent their co-evolution through similar processes of adsorption and desorption from Fe (hydr)oxides surfaces. The third PC for the pre-monsoon accounts for 17.5% of the overall variance. It is positively loaded by NO_3^- and negatively loaded by PO_4^{3-} and may represent anthropogenic inputs to the groundwater.

In the post-monsoon season, the first PC is loaded by TDS, EC, Ca^{2+}, Mg^{2+}, Cl^- and NO_3^- and has accounts for 36.0% of the overall variance (Table 4). Carbonate weathering appears to be more dominating in the post-monsoon season due to the dissolution effect of precipitation, while mobilization of NO_3^- and Cl^- from anthropogenic sources such as sewage could account for their

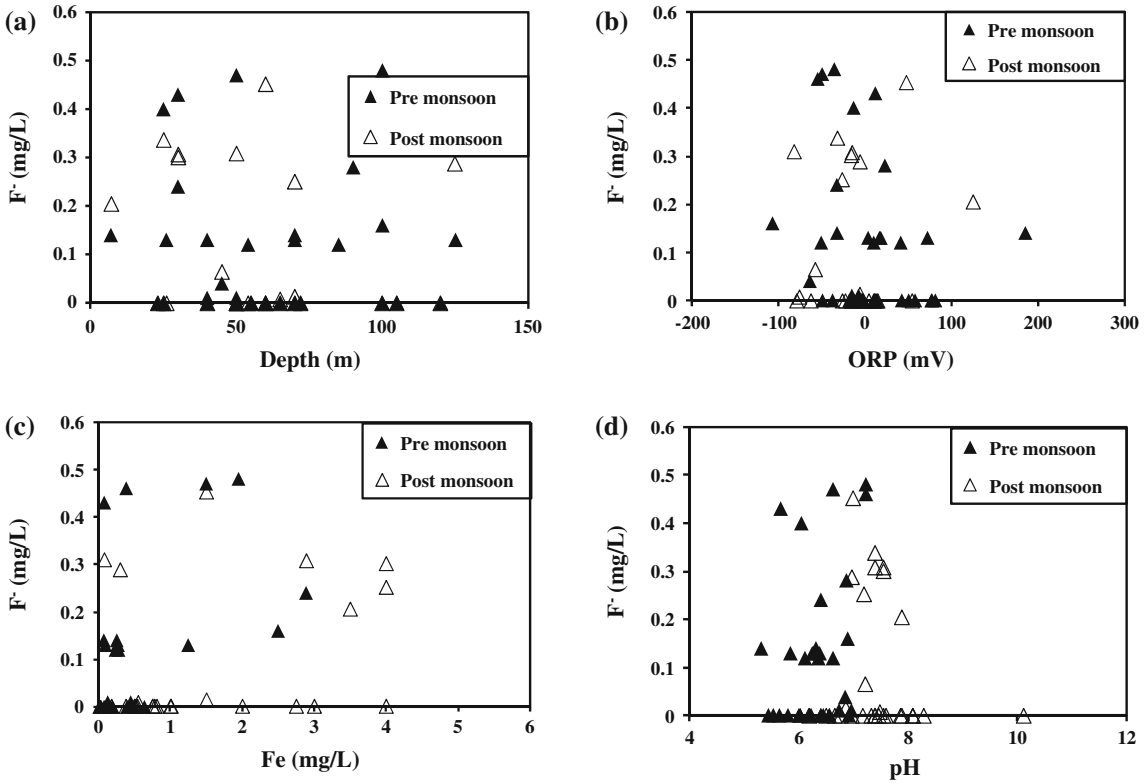

Fig. 8 Comparison of F^- behavior with other parameters spatially and seasonally. **a** F^- versus depth, **b** F^- versus ORP, **c** F^- versus Fe, **d** F^- versus pH

Table 4 Principle component analyses (PCA) of the chemical parameters in the groundwater of the pre- and post-monsoon seasons

Parameters	Pre-monsoon			Post-monsoon		
	PC1	PC2	PC3	PC1	PC2	PC3
TDS	0.79			0.94		
pH	0.77				0.74	
ORP	−0.72					0.70
EC	0.65			0.94		
Na^+						0.86
K^+	0.84					0.83
Ca^{2+}		0.87		0.95		
Mg^{2+}		0.90		0.96		
Cl^-	0.60			0.95		
SO_4^{2-}		0.91				
PO_4^{3-}			−0.73			0.81
NO_3^-			0.75	0.85		
HCO_3^-	0.77				0.82	
F^-		0.91				
As	0.61				0.94	
Fe	0.68				0.84	
% Variance	40.89	22.49	17.45	35.96	22.49	16.04

high loadings. The second PC is loaded by pH, HCO_3^-, As and Fe, and accounts for 22.5% of the variance. This reflects co-evolution of Fe and As from Fe-rich complexes and the alkaline environment promotes As release (Smedley and Kinniburgh 2002; Kim et al. 2012). The third PC is loaded by ORP, Na^+, K^+, and PO_4^{3-}, accounting for 16.0% of the overall variance. This component is likely controlled by silicate weathering and redox-driven PO_4^{3-} release to the groundwater of the region.

Hierarchical cluster analysis

In samples from the pre-monsoon season, SO_4^{2-} and F^- are clustered (Fig. 9a), which could be attributed to their similar adsorption and desorption behaviors. Silicate weathering and anthropogenic activities may control the cluster represented by TDS, Cl^-, EC, NO_3^-, Na^+ and K^+. Clustering of As, Fe, pH, and HCO_3^- supports involvement of Fe (hydr)oxides, alkalinity, and resulting increases in pH in As mobilization.

Clustering of Ca^{2+} and Mg^{2+} suggests carbonate weathering as the source of the two cations. Phosphate is also in this cluster and may indicate alternative sources of

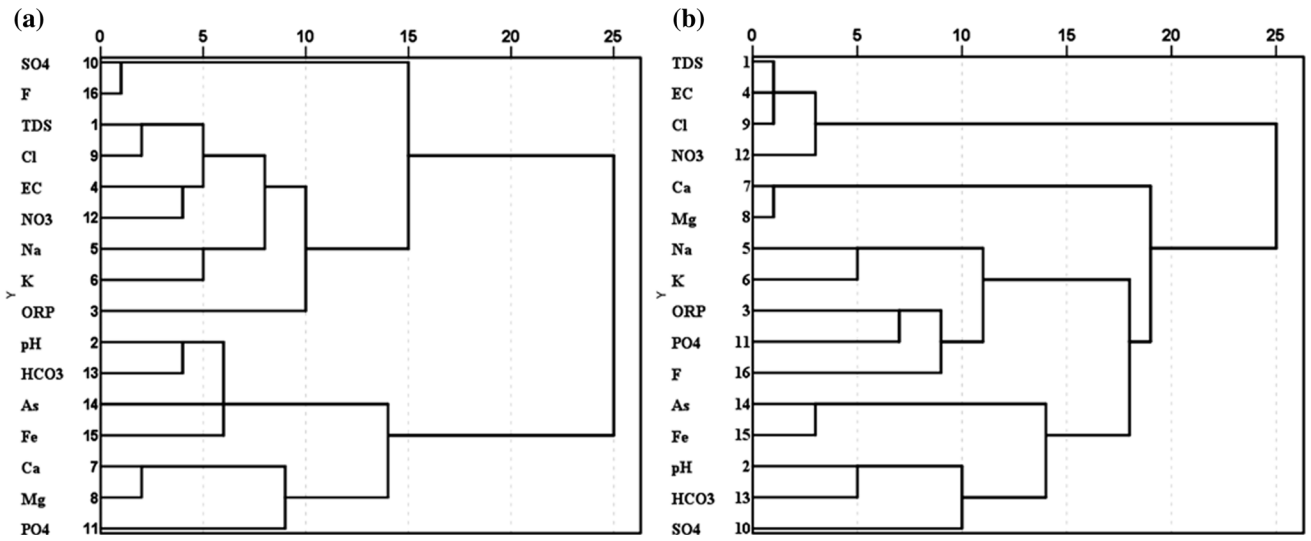

Fig. 9 Hierarchical cluster analysis during **a** pre-monsoon and **b** post-monsoon seasons

Table 5 Saturation indices obtained by speciation modeling in the pre-monsoon season

Mineral phase	Samples											
	T3	T9	T10	T14	T16	T42	T45	T50	T55	T56	T57	T63
Aragonite	−1.58	−2.34	−1.88	−1.60	−0.93	−2.00	−2.76	−2.40	−0.48	−1.08	−0.37	−1.09
Arsenolite	−13.21	−13.40	−13.44	−12.97	−14.35	−14.31	−13.96	−13.71	−14.77	−12.69	−13.36	−13.15
As_2O_5	−36.41	−32.65	−31.76	−34.24	−36.59	−33.35	−36.47	−36.55	−36.14	−38.95	−33.48	−36.57
Calcite	−1.44	−2.19	−1.73	−1.46	−0.78	−1.85	−2.62	−2.25	−0.33	−0.94	−0.23	−0.94
Claudetite	−13.25	−13.44	−13.48	−13.01	−14.39	−14.35	−14.00	−13.75	−14.81	−12.73	−13.40	−13.19
Dolomite (disordered)	−3.53	−5.29	−4.38	−3.46	−2.25	−4.46	−5.87	−5.22	−0.88	NF	−0.98	−2.31
Dolomite (ordered)	−2.98	−4.74	−3.83	−2.91	−1.70	−3.91	−5.32	−4.67	−0.33		−0.43	−1.76
$Fe(OH)_2$ (am)	−5.09	NF	NF	NF	−4.74	NF	NF	−7.90	−4.34	−4.21	−3.67	−4.95
$Fe(OH)_2$(c)	−4.49	NF	NF	NF	−4.14	NF	NF	−7.30	−3.74	−3.61	−3.07	−4.35
Gypsum	−2.87	−3.07	−3.08	−2.85	−2.54	−2.99	−3.14	−3.25	−3.07	−3.48	−3.06	−2.55
Halite	−8.48	−8.36	−8.47	−8.00	−8.72	−8.50	−7.59	−8.27	−8.84	−3.13	−8.24	−8.08
Mirabilite	−9.95	−10.28	−9.78	−10.15	−10.75	−9.93	−9.18	−10.07	−10.16	−8.83	−9.68	−9.84
Siderite	−0.53	NF	NF	NF	−0.88	NF	NF	−3.03	−0.24	0.42	0.63	−0.29
$Fe(OH)_2.7Cl._3$(s)	NF	6.19	6.43	7.62	NF	6.18	5.80	NF	NF	NF	NF	NF
$Fe_2(SO_4)_3$(s)	NF	−30.99	−32.04	−31.91	NF	−33.81	−32.20	NF	NF	NF	NF	NF
$FeAsO_4$:$2H_2O$(s)	NF	−7.68	−6.79	−6.92	NF	−7.77	−10.02	NF	NF	NF	NF	NF
Ferrihydrite	NF	2.59	3.04	4.15	NF	2.85	2.16	NF	NF	NF	NF	NF
Ferrihydrite (aged)	NF	3.10	3.55	4.66	NF	3.36	2.67	NF	NF	NF	NF	NF
Geothite	NF	5.30	5.75	6.85	NF	5.56	4.87	NF	NF	NF	NF	NF

am, c and s stand for amorphous, crystalline, and solid, respectively

NF here stands for 'not found'

Ca^{2+}, such as apatite. TDS, EC, Cl^- and NO^{3-} are clustered together in the post-monsoon (Fig. 9b). This reflects weathering and dissolution of salts, and possibly mobilization of previously static anthropogenic influxes, under the influence of precipitation. Clustering of Ca^{2+} and Mg^{2+} reflects carbonate weathering under the high precipitation of the post-monsoon. Sodium and K^+ reflect silicate weathering which is enhanced in the post-monsoon. Phosphate, ORP, and F^- also form a cluster, while As and Fe are clustered together because Fe (hydr)oxides are the common source of both As and Fe. The cluster of Fe and As is near the cluster of pH, $HCO_3^-$and SO_4^{2-}, consistent

Table 6 Saturation indices obtained by speciation modeling in the post-monsoon season

Mineral phase	Samples											
	T3	T9	T10	T14	T17	T18	T45	T51	T54	T55	T57	T63
Aragonite	−0.39	−0.46	−0.62	−0.44	−1.15	−0.47	−0.75	0.45	−19.59	0.25	0.25	−0.72
Arsenolite	−17.19	−17.11	−13.42	−15.86	−18.40	−20.25	−19.77	−26.21	−7.66	−16.59	−13.12	−16.81
As_2O_5	−34.65	−33.59	−33.00	−33.62	−34.03	−33.55	−35.20	−38.71	−33.67	−35.95	−34.63	−38.77
Calcite	−0.25	−0.32	−0.48	−0.30	−1.00	−33.55	−0.61	0.60	−0.42	0.40	0.39	−0.58
Claudetite	−17.23	−17.15	−13.46	−15.90	−18.44	−20.29	−19.81	−26.25	−19.63	−16.63	−13.16	−16.85
Dolomite (disordered)	−1.07	−1.44	−1.61	−1.23	−2.51	−1.25	−1.82	0.70	−1.56	0.52	−0.01	−1.85
Dolomite (ordered)	−0.52	−0.89	−1.06	−0.68	−1.96	−0.70	−1.27	1.25	−1.01	1.07	0.54	−1.30
$Fe(OH)_2$ (am)	−2.71	NF	NF	−2.58	NF	NF	−2.35	−3.06	NF	−2.35	−1.81	−4.37
$Fe(OH)_2$(c)	−2.11	NF	NF	−1.98	NF	NF	−1.75	−2.46	NF	−1.75	−1.21	−3.77
Gypsum	−3.09	−1.90	−2.93	−3.22	−3.48	−3.26	−3.54	−25.02	NF	−3.14	−3.15	−3.17
Halite	−6.95	−8.46	−8.19	−7.75	−9.23	−7.94	−7.36	−3.20	NF	−8.38	−8.05	−8.02
Mirabilite	−9.84	−8.84	−9.71	−9.48	−11.93	−9.45	−9.11	−10.00	NF	−10.26	−9.36	−9.80
Siderite	0.93	NF	NF	1.07	NF	NF	0.80	−0.54	NF	1.05	1.71	−0.81
$Fe(OH)_2.7Cl._3$(s)	NF	8.63	7.95	NF	8.58	8.20	NF	NF	8.91	NF	NF	NF
$Fe_2(SO_4)_3$(s)	NF	−32.34	−34.65	NF	−36.45	−37.02	NF	NF	NF	NF	NF	NF
$FeAsO_4{:}2H_2O$(s)	NF	−5.09	−5.65	NF	−5.39	−5.55	NF	NF	−5.04	NF	NF	NF
Ferrihydrite	NF	5.66	4.80	NF	5.57	5.17	NF	NF	5.74	NF	NF	NF
Ferrihydrite (aged)	NF	6.17	5.31	NF	6.08	5.68	NF	NF	6.25	NF	NF	NF
Geothite	NF	8.36	7.51	NF	8.28	7.88	NF	NF	8.45	NF	NF	NF

am, c and s stand for amorphous, crystalline, and solid, respectively

NF here stands for 'not found'

with greater As release in an alkaline environment, while SO_4^{2-} is a competitive anion for adsorption on Fe (hydr)oxide surfaces.

Speciation

Speciation analysis can be used to determine the various aqueous phases or species affecting groundwater, based on saturation indices (SI) (Kumar et al. 2010a). Speciation was determined for representative samples of each season (Tables 5, 6). As phases (arsenolite, As_2O_5, claudetite and $FeAsO_4{\cdot}2H_2O$) were undersaturated in the groundwater in both seasons. SI values were lower in the post-monsoon season than in the pre-monsoon, perhaps due to dilution resulting from precipitation. The mineral siderite ($FeCO_3$) was undersaturated in pre-monsoon samples but the condition tends to reverse in the post-monsoon as SI increases.

The tendency of minerals to precipitate increases with increasing SI. Siderite may be one of the phases that precipitate during pre- and post-monsoon seasons and form coatings on primary minerals such as geothite and ferrihydrite, decreasing their tendency to dissolve (Vencelides et al. 2007; Kumar et al. 2010a) (Tables 5, 6). Iron (II) hydroxide [$Fe(OH)_2$] (amorphous and crystalline) is more undersaturated in the pre-monsoon than in the post-monsoon, indicating greater dissolution in the post-monsoon. Aragonite, calcite, and dolomite have higher SIs in the post-monsoon, indicating movement toward saturation, consistent with greater weathering and dissolution than in the pre-monsoon.

Although low SI values of groundwater As suggest that its level may remain low, other factors need to be considered as well. As contamination of groundwater is likely to increase, based on undersaturation by As-bearing phases, although primary minerals such as goethite and ferrihydrite can provide sinks for both F^- and As. Yet the prevalent reducing conditions would continue to promote dissolution and further increases in As in the groundwater. Anthropogenic influences such as excessive pumping leads to drawdown, which can affect deeper aquifers and the groundwater As levels. Another important factor which could influence the future groundwater As is overuse of phosphate fertilizers and arsenical pesticides.

Conclusion and recommendation

Weathering and dissolution of calcite and silicate appear to control the overall hydrogeochemistry of the BFP region. The aquifer system is mixed, with both reducing and

oxidizing conditions, but reducing conditions are predominant. Arsenic and Fe showed a strong positive correlation, likely due to reductive dissolution of Fe (hydr)oxides and As release with increasing pH. Fluoride and SO_4^{2-} are also clustered in the pre-monsoon season, indicating their similar desorption characteristics. The process of reductive dissolution Fe (hydr)oxide prevails throughout the year as As and Fe were clustered in both seasons. Aquifer recharge during the post-monsoon could lead to saturation of the vadose zone, creating more reducing conditions, which favors higher As levels. The higher pH in the post-monsoon also may be influencing reductive dissolution of Fe (hydr)oxides and As release as the point of zero charge is approached or exceeded. Fluoride-bearing minerals appear to be the primary source of F^-, but Fe (hydr)oxides may be a secondary source of F^-, as suggested by the positive correlation between As and F^- in the pre-monsoon season.

This study can be improved by increasing the sampling density. The influences of anthropogenic activities on As and F^- levels in groundwater can be studied by intensive localized sampling in smaller regions of the BFP. To gain a better understanding of the role of the river and fluvial environment on As and F^- levels in groundwater, comparative sampling should be carried out in areas outside the BFP, especially in arid regions which lack fluvial conditions. Isotope tracer techniques can be used to identify groundwater As and F^- flow paths and recharge routes. They in turn can be used to identify As hotspots and F^--enriched aquifers. This can be helpful in delineating groundwater for human consumption with safe levels of As and F^-, and for identifying areas where treatment or better management are needed.

Acknowledgements This work is funded by Science and Engineering Research Board (SERB), the Department of Science and Technology (DST), under the Govt. of India under the Fast Track Young Scientist Scheme awarded to Dr. Manish Kumar (SR/TP/ES-32/2012). Nilotpal Das likes to thank the assistance received from Council for Scientific and Industrial Research (CSIR)—India, for financial assistance as JRF [09/796(0052)/2012-EMR-1]. We acknowledge the help received for the cation analysis by IC, to the project "Physico-chemical characterization of aerosol and source apportionment in the mid-Brahmaputra plain in Assam: A modeling approach" funded by the Ministry of Earth Sciences, India: MoES/16/16/10-RDEAS.

References

Ahmed KM, Bhattacharya P, Hasan MA, Akhter SH, Alam SM, Bhuyian MH, Imam MB, Khan AA, Sracek O (2004) Arsenic enrichment in groundwater of the alluvial aquifers in Bangladesh: an overview. Appl Geochem 19:181–200

APHA (2005) Standard methods for the examination of water and wastewater, 19th edn. American Public Health Association, Washington

Arveti N, Sarma MR, Aitkenhead-Peterson JA, Sunil K (2011) Fluoride incidence in groundwater: a case study from Talupula, Andhra Pradesh, India. Environ Monit Assess 172:427–443

Balasundaram MS (1977) Contribution to geomorphology and geohydrology of the Brahmaputra valley. Geol Surv India

Bhattacharya P, Frisbie SH, Smith E, Naidu R, Jacks G, Sarkar B (2002) Arsenic in the environment: a global perspective. Handbook of heavy metals in the environment. Marcell Dekker Inc., New York, pp 147–215

Bhattacharya R, Jana J, Nath B, Sahu SJ, Chatterjee D, Jacks G (2003) Groundwater As mobilization in the Bengal Delta Plain, the use of ferralite as a possible remedial measure a case study. Appl Geochem 18:1435–1451

Bhuyan B, Bhuyan D (2011) Groundwater arsenic contamination status in Dhakuakhana sub-division of Lakhimpur district, Assam, India. ActachimicapharmaIndica 1:14–19

Brindha K, Rajesh R, Murugan R, Elango L (2011) Fluoride contamination in groundwater in parts of Nalgonda district, Andhra Pradesh, India. Environ Monit Assess 172:481–492

Brunt R, Vasak L, Griffioen J (2004) Fluoride in groundwater: probability of occurrence of excessive concentration on global scale. IGRAC

Bundschuh J, Farias B, Martin R, Storniolo A, Bhattacharya P, Cortes J, Bonorino G, Albouy R (2004) Groundwater arsenic in the Chaco-Pampean plain, Argentina: case study from Robles county, Santiago del Estero province. Appl Geochem 19:231–243

Chakraborti D, Chanda CR, Samanta G, Chowdhury UK, Mukherjee SC, Pal AB, Sharma B, Mahanta KJ, Ahmed HA, Sing B (2000) Fluorosis in Assam, India. Curr Sci 78:1421–1423

Chen K, Jiao JJ, Huang J, Huang R (2007) Multivariate statistical evaluation of trace elements in groundwater in a coastal area in Shenzhen, China. Environ Pollut 147:771–780

Critto A, Carlon C, Marcomini A (2003) Characterization of contaminated soil and groundwater surrounding an illegal landfill (S. Giuliano, Venice, Italy) by principal component analysis and kriging. Environ Pollut 122:235–244

Das BK, Kaur P (2001) Major ion chemistry of Renuka lake and weathering processes, Sirmaur district, Himachal Pradesh, India. Environ Geol 40:908–917

Das B, Talukdar J, Sarma S, Gohain B, Dutta RK, Das HB, Das SC (2003) Fluoride and other inorganic constituents in groundwater of Guwahati, Assam, India. Curr Sci Bangalore 85:657–660

Evans P (1964) The tectonic framework of Assam. J GeolSoc India 5:80–96

Fisher RS, Mullican WF III (1997) Hydrochemical evolution of sodium-sulfate and sodium-chloride groundwater beneath the northern Chihuahuan Desert, Trans-Pecos, Texas, USA. Hydrogeol J 5:4–16

Ghosh NC, Singh RD (2009) Groundwater Arsenic Contamination in India: vulnerability and Scope for Remedy. NIH, Roorkee

Gibbs RJ (1970) Mechanisms controlling world water chemistry. Science 170:1088–1090

Halim MA, Majumder RK, Nessa SA, Hiroshiro Y, Sasaki K, Saha BB, Saepuloh A, Jinno K (2010) Evaluation of processes controlling the geochemical constituents in deep groundwater in Bangladesh: spatial variability on arsenic and boron enrichment. J Hazard Mater 180:50–62

Harvey CF, Swartz CH, Badruzzaman AB, Keon-Blute N, Yu W, Ali MA, Jay J, Beckie R, Niedan V, Brabander D, Oates PM (2005) Groundwater arsenic contamination on the Ganges Delta: biogeochemistry, hydrology, human perturbations, and human suffering on a large scale. ComptesRendus. Geoscience 337:285–296

Heroy DC, Kuehl SA, Goodbred SL (2003) Mineralogy of the Ganges and Brahmaputra Rivers: implications for river switching and late quaternary climate change. Sed Geol 155:343–359

Huizing HG (1971) A reconnaissance study of the mineralogy of sand fractions from East Pakistan sediments and soils. Geoderma 6:109–133

Jain KS, Agarwal PK, Singh VP (2007) Hydrology and water resources of India. Water SciTechnol Library Springer 57:419–472

Kim SH, Kim K, Ko KS, Kim Y, Lee KS (2012) Co-contamination of arsenic and fluoride in the groundwater of unconsolidated aquifers under reducing environments. Chemosphere 87:851–856

Kumar M, Ramanathan AL, Rao MS, Kumar B (2006) Identification and evaluation of hydrogeochemical processes in the groundwater environment of Delhi, India. Environ Geol 50:1025–1039

Kumar M, Kumari K, Singh UK, Ramanathan AL (2008) Hydrogeochemical processes in the groundwater environment of Muktsar, Punjab: conventional graphical and multivariate statistical approach. Environ Geol 57:873–884

Kumar M, Kumar P, Ramanathan AL, Bhattacharya P, Thunvik R, Singh UK, Tsujimura M, Sracek O (2010a) Arsenic enrichment in groundwater in the middle Gangetic Plain of Ghazipur District in Uttar Pradesh, India. J Geochem Explor 105:83–94

Kumar P, Kumar M, Ramanathan AL, Tsujimura M (2010b) Tracing the factors responsible for arsenic enrichment in groundwater of the middle Gangetic Plain, India: a source identification perspective. Environ Geochem Health 32:129–146

Liao CM, Lin TL, Chen SC (2008) A Weibull-PBPK model for assessing risk of arsenic-induced skin lesions in children. Sci Total Environ 392:203–217

Mahanta C (1995) Distribution of nutrients and toxic metals in the Brahmaputra River Basin. Ph.D thesis Jawaharlal Nehru University, India

Mithal RS, Srivastava LS (1959) Geotectonic positions and earthquakes of Ganga-Brahmaputra region. In: Proceedings of the first symposium on earthquake engineering. University of Roorkee, Roorkee, India

Mukherjee A, Sengupta MK, Hossain MA, Ahamed S, Das B, Nayak B, Lodh D, Rahman MM, Chakraborti D (2006) Arsenic contamination in groundwater: a global perspective with emphasis on the Asian scenario. J Health Popul Nutr 24:142–163

Pillai KS, Stanley VA (2002) Implications of fluoride an endless uncertainty. J Environ Biol Acad Environ Biol India 23:81–87

Piper AM (1953) A graphic procedure for the geo-chemical interpretation of water analysis. USGS groundwater. Note 12

Rajmohan N, Elango L (2004) Identification and evolution of hydrogeochemical processes in theground water environment in an area of the Palar and Cheyyar River Basins, Southern India. Environ Geol 46:47–61

Reddy DP (2012) Arsenic and iron contamination in ground water in lower Brahmaputra Basin in Bongaigaon and part of Dhubri Districts of Assam State. India Water Week-Water, Energy and Food Security, India

Reddy AG, Reddy DV, Rao PN, Prasad KM (2010) Hydrogeochemical characterization of fluoride rich groundwater of Wailpalli watershed, Nalgonda District, Andhra Pradesh, India. Environ Monit Assess 171:561–577

Saxena V, Ahmed S (2001) Dissolution of fluoride in groundwater: a water–rock interaction study. Environ Geol 40:1084–1087

Saxena V, Ahmed S (2003) Inferring the chemical parameters for the dissolution of fluoride in groundwater. Environ Geol 43:731–736

Singh AK (2004) Arsenic contamination in groundwater of North Eastern India. In: 11th national symposium on hydrology with focal theme on water quality. National Institute of Hydrology Roorkee, proceeding, Vol 255262

Smedley PL, Kinniburgh DG (2002) A review of the source, behaviour and distribution of arsenic in natural waters. Appl Geochem 17:517–568

Smedley PL, Nicolli HB, Macdonald DM, Barros AJ, Tullio JO (2002) Hydrogeochemistry of arsenic and other inorganic constituents in groundwaters from La Pampa, Argentina. Appl Geochem 17:259–284

Smedley PL, Zhang M, Zhang G, Luo Z (2003) Mobilisation of arsenic and other trace elements in fluviolacustrine aquifers of the Huhhot Basin, Inner Mongolia. Appl Geochem 18:1453–1477

Susheela AK (2001) Fluorosis: Indian scienario: a treatise on fluorosis. Fluorosis Research and Rural Development Foundation, Delhi

Tapponier P, Molnar P (1977) Active faulting and Cenozoic tectonics of China. J Geophys Res 82:2905–2930

Vencelides Z, Sracek O, Prommer H (2007) Modelling of iron cycling and its impact on the electron balance at a petroleum hydrocarbon contaminated site in Hnevice, Czech Republic. J Contam Hydrol 89:270–294

World Health Organization (WHO) (2008) Guidelines for drinking-water quality: incorporating first and second addenda to 3rd edn, vol 1, Recommendations